

## Development of Vulnerability Model for Industrial Buildings to Extreme Wind Loading for Cyclonic Regions

K.M.C.Konthesingha<sup>1</sup>, M.G.Stewart<sup>2</sup>, J. Ginger<sup>3</sup> and D.Henderson<sup>4</sup>

<sup>1,2</sup>Centre for Infrastructure Performance and Reliability  
The University of Newcastle, Australia

<sup>3,4</sup>Cyclone Testing Station  
James Cook University, Townsville, Australia

### Abstract

A vulnerability model is being developed to predict the probability and extent of damage to metal-clad industrial buildings (industrial sheds) due to extreme wind loading. Structural reliability-based methods that describe the spatially distributed wind load and component/connection strengths probabilistically were used in this model. Two main failure mechanisms in the roof envelop namely; failure of roof cladding and purlin failure were considered for this model. Interdependency between the failure mechanisms, load sharing effect due to connection/component failure and internal pressure variation due to roof cladding failure are also incorporated. Wind vulnerability of a hot rolled structural steel, metal-clad, gable-end, typical shed designed for cyclonic region in Australia is investigated. The large variation in vulnerability of the shed with the incorporation cyclone washers and/or internal pressure (e.g. an open door) is highlighted.

### Introduction

Past extreme wind events such as cyclones and hurricanes have shown that it is one of the main natural hazards that cause damage to buildings and result in large economic losses (Holmes, 2007). The prediction of damage to the buildings from these extreme wind events is essential to develop policies to effectively reduce economic losses. Wind vulnerability models are used to predict the probability of damage to buildings and their contents due to wind loading. Vulnerability models play a key role in cost-benefit analysis which contributes to developing design procedures and other mitigation strategies to reduce economic losses due to severe wind events (e.g., Stewart et al. 2014, Stewart 2014). The models can be developed either by fitting curves to the damage data from historical wind damage records and insurance data (i.e. empirical models) or by using engineering knowledge to obtain the damage due to wind loading by investigating the behaviour of buildings and its components (i.e. engineering models).

In the current study, an engineering vulnerability model is developed based on structural reliability, spatial, and probabilistic analysis for metal clad industrial buildings against wind loading. Roof envelop failure is considered in this model which include two main failure mechanisms (i) roof cladding pulling over fixing and (ii) purlin failure (i.e. purlin to rafter connection failure and/or purlin buckling failure). The external pressure coefficients for the model are obtained from wind tunnel testing. The vulnerability curves for representative industrial sheds (i.e. hot rolled structural steel, metal-clad, gable-end, industrial shed) designed to current Australian building standards in cyclonic regions in Australia (North Queensland) are generated considering the effect of roof cyclone washers and dominant openings. Experience in recent cyclones in Australia suggests that some roller doors fail at their connections to the building,

thus causing a dominant opening leading to damage of the building (Henderson and Ginger, 2008).

In this model, load redistribution after connection/component failure is incorporated based on the progressive failure load paths which allows the failure of each roof sheet to be modelled. Internal pressure is incorporated in this vulnerability model as a function of dominant opening, created by failed roof sheets due to wind load. The interdependency of the component failure is also considered in this model.

### Model Development

Industrial buildings with spans (D) of 20 m to 40 m, lengths of 50 m or more, heights of 5 m to 10 m, and gable-end low pitch (less than 10°) roofs are used in industrial applications in Australia. The structural systems of these buildings generally consist of portal or pin-jointed frames, spaced at 4 m to 8 m along the length of the building. Metal sheet cladding is attached to roof purlins and wall girts using fasteners. Cross-bracing between the end frames resist longitudinal (i.e. in direction of ridge-line) wind loads.

Details of a representative hot rolled structural steel, low-pitch roof, metal-clad, metal-framed industrial building in cyclonic regions in Australia are shown in Figure 1 and is used in investigating the wind vulnerability in this study. These details are obtained from a survey carried out by the CTS, described in Leitch et al. (2006). The industrial building is designed with a dominant opening on the windward wall and consists of eleven portal frames. The purlin type Z25019 is used here. Metal cladding with a thickness of 0.48 mm is used for the roof. Width of the cladding is 762 mm and a single sheet is laid from eave to ridge of the roof (length=18.6 m). Four fasteners along the cladding width per sheet were considered. Purlins are equally spaced with 1300 mm spacing (Figure 1b) except for the first span in each side of the roof. As an enhancement strategy against cyclonic loading, an additional purlin is introduced near each eave, in between the first two purlins as shown in Figure 1b. The total number of fasteners in a roofing sheet is 64 and the total number of roof sheets used in the industrial building is 150.

The two failure mechanisms, cladding pulling over fixing and purlin failure (i.e. purlin to rafter connection failure and/or purlin buckling failure) are considered (i.e. roof envelop failure) in this study. The wind load and component/connection strengths are obtained probabilistically and are described in the subsequent sections.

### Limit State

The limit state of roof failure is defined as wind load exceeding the component/connection capacity. Roof cladding pulling over fixing failure occurs when the internal and external pressures are adequate to cause uplift of the roof cladding from the fastener. The limit state function  $G(x)$  is:

$$G(x) = R - (W - D) \quad (1)$$

where R is the actual component strength of each failure mode, W is the actual wind load and D the actual dead load. The component/connection failure occurs when  $G(x) < 0$ . Event-based Monte-Carlo simulation methods are used in this model to obtain the probability of failure of each connection with increasing wind load.

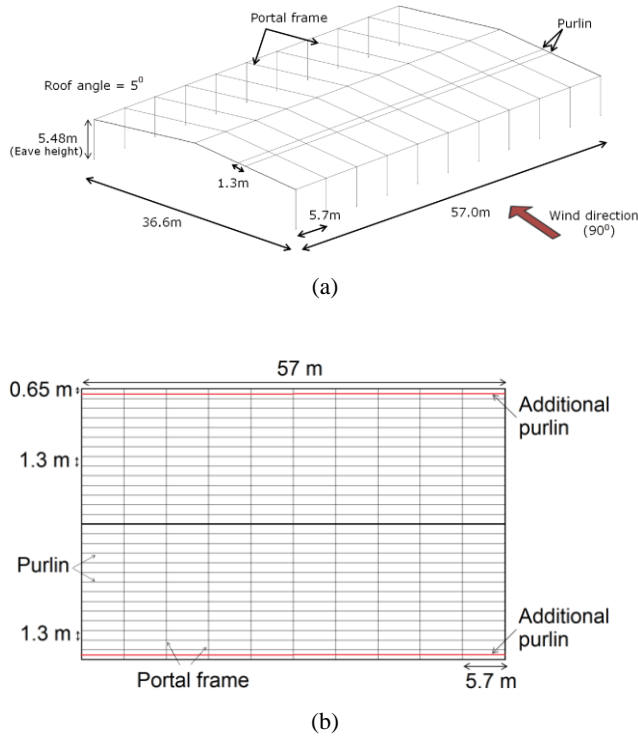


Figure 1. Shed details (a) Overall dimensions (b) Plan view of the roof with purlin arrangement

### Probabilistic Model for Wind Load

The wind load (W) was calculated probabilistically as (Holmes 1985, Pham 1985):

$$W = BV^2 \quad (2)$$

where V is the maximum gust velocity at 10 m height in terrain category 2. The parameter B is:

$$B = \lambda \cdot A \cdot (C \cdot E^2 \cdot D^2 \cdot G \cdot \frac{\rho}{\rho_N}) \quad (3)$$

where C is the quasi-steady pressure coefficient, E is a velocity height multiplier that accounts for the exposure and height of the building considered, D is a factor for wind directionality effects, G is a factor for gusting effects (related to  $K_a$  and  $K_1$ ),  $\rho$  is the density of air, A is the tributary area, and  $\lambda$  is the factor accounting for modelling inaccuracies and uncertainties in analysis methods. The variables within brackets in Equation (3) are directly related to the nominal values given in the Australian wind loading standard AS/NZS 1170.2 (2011).

External pressure coefficients ( $C_{pe}$ ) and internal pressure coefficients ( $C_{pi}$ ) are used for the quasi-steady pressure coefficient (C) in the above equation. The external pressure coefficients ( $C_{pe}$ ) are obtained from wind tunnel testing. Based on the analysis of the industrial buildings surveyed by the CTS, a set of representative wind tunnel model results for the wind direction  $90^\circ$  are obtained from the United States National Institute of Standards and Technology (NIST) aerodynamics database. The NIST database provides time histories of external pressures

measured on the roof and walls of a series of low-rise building configurations at a length scale of 1/100 in the wind tunnel at the University of Western Ontario. Figure 2 shows the pressure tap locations of the wind tunnel model considered for the current study.

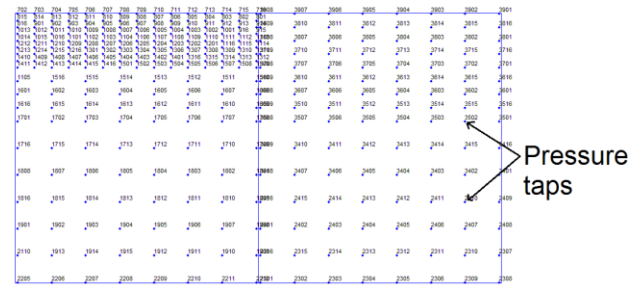


Figure 2. Pressure tap locations

The wind loading model utilises data from pressure taps located 5.7 m and 2.6 m apart (i.e. rafter spacing and double purlin spacing). The pressure values are modified with a gust factor of 1.62. Figure 3 shows the pressure coefficient distribution for the wind direction  $90^\circ$  on the roof of the industrial building, obtained from the wind tunnel tests.

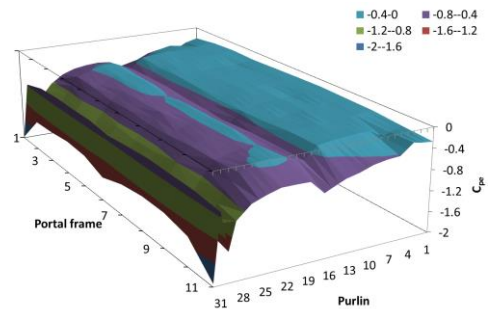


Figure 3. Pressure variation on the roof for the wind direction  $90^\circ$

The wind tunnel pressure coefficient data are assumed to have an Extreme Value Type 1 (Gumbel) probability distribution. The other variables in Equation (3) are assumed to have a log-normal probability distribution with estimated means and coefficient of variations (COV) given in Table 1 derived from Henderson and Ginger (2007) for their vulnerability model of Australian high-set houses. They deduced those data from surveys and other studies (Pham et al 1983, Holmes 1985). The subscript 'N' denoted in Table 1 is the nominal (design) value of the respective parameter obtained from the Australian wind loading standard AS/NZS 1170.2 (2011), and  $A_N$  is obtained by calculating the effective tributary area of each component/connection. The nominal air density ( $\rho_N$ ) is  $1.2 \text{ kg/m}^3$ .

Parameter	Mean	COV
$\lambda/\lambda_N$	1	0.05
$A/A_N$	0.92	0.1
$E/E_N$	0.95	0.1
$D/D_N$	0.9	0.1
$G/G_N$	0.95	0.1
$\rho/\rho_N$	1	0.02

Table1. Parameters for wind loading

Internal pressure coefficients are obtained from the wind loading standard (AS/NZS 1170.2-2011) and are changed according to the presence or absence of a windward dominant opening. The internal pressure variation caused by the roof sheeting failure is also incorporated in this model. It is done by reducing the internal pressure coefficients depending on the number of failed roof sheets. Here the internal pressure is assumed as a function of dominant opening created by the failed roof sheets due to

wind load. Figure 4 shows the internal pressure variation assumed for the industrial building with the conditions namely building with and without dominant opening. It is assumed to vary in a liner function until four roof sheets fail and then considered unchanged thereafter. Equations of the liner functions are also shown in Figure 4.

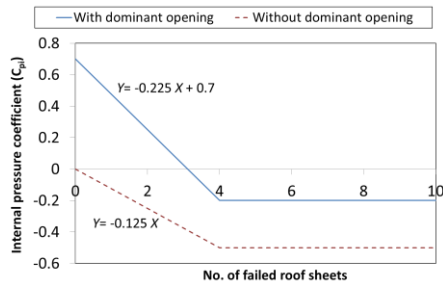


Figure 4. Internal pressure coefficient variation for building with and without a dominant opening on the windward wall

### Probabilistic Model for Roof Cladding (Sheet) Failure

The probabilistic model for roof cladding pulling over the fixing is obtained from expert judgment and component testing at the Cyclone Testing Station (CTS) at James Cook University. Roof metal cladding with a thickness of 0.48 mm is used in the industrial building investigated in this study. Due to the different number of load cycles affecting different parts of the roof, fixing capacities are lower for edge and corner regions of the roof. The different pressure zones for the industrial shed are shown Figure 5. Three pressure zones were considered according to AS4055 (2012) and AS/NZS1170.2 (2011).

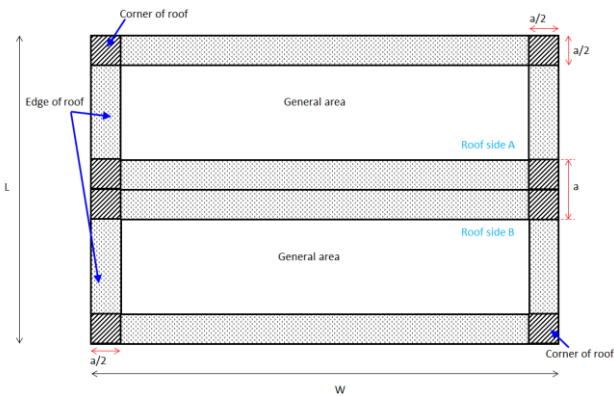


Figure 5. Plan view of the roof with different pressure zones ( $a=6300$  mm)

The mean strengths for cladding pulling over the fixing of the roof sheet have been derived from experimental testing (Henderson 2010), and damage assessments for different roof zones with and without cyclone washers fitted in the roof. These strengths were assumed to have lognormal distributions (Henderson and Ginger 2005). The coefficient of variation is assumed as 30%.

Vulnerability curves in this study are developed based on roof sheet failure. The roof sheet failure definition is based on the number of fasteners failed in each roof sheet. This fastener failure percentage value is an input variable in the model and the results presented in this paper are based on 20% (i.e. a roof sheet with 20% of the fasteners failed is considered as failed). The number of fasteners in a roofing sheet depends on the type of roofing sheet used and fasteners spacing. The model is capable of developing vulnerability curves of any type of roofing sheet used in industrial buildings.

### Probabilistic Model for Purlin Failure

The probabilistic model for purlin failure (i.e. purlin to rafter connection failure and/or purlin buckling failure) is obtained by

referring to the literature, including capacity tables for purlin design in this study. Purlin capacity tables are based on a finite element flexural torsional buckling analysis for modelling the whole purlin system. Note that all design calculations are in accordance with the Australian Standard for Cold Formed Structures AS/NZS 4600 (1996), and design capacities include not only failure loads of purlins, but also their connection to the supporting rafter.

Clarke and Hancock (1999) compared test results with ultimate load capacities of purlins derived from AS/NZS 4600 (1996). The model error (test failure load divided predicted capacity) for a finite element lateral buckling analysis was a mean of 1.27 and a COV of 0.13, for a triple span purlin with one row of bridging and uplift loads.

The nominal (design) uplift capacity for a Z25019 purlin three-lapped span with one or two rows of bridging is  $R_n=6.93$  kN/m (Lysaght 2008) assuming a capacity reduction factor of 0.9. The mean to nominal capacity is a function of model error, ratio of actual to nominal yield stress, and ratio of actual thickness to nominal thickness. Using statistics from Clarke and Hancock (1999) and Pham and Hancock (2009), the mean resistance ( $R$ ) is 9.42 kN/m with a COV of 0.13. It is assumed that the distribution of purlin capacity is lognormally distributed.

### Load Sharing and Interdependency

Henderson (2010) found that when a particular fastener fails, its load is redistributed to the adjacent fasteners as shown in Figure 6. This load redistribution mechanism is adopted in the current vulnerability model to share the failure load of a connection with adjacent connections. As shown in Figure 6, when the fastener 'A' fails, 90% of its load at the time of failure is shared with adjacent fasteners 'B' and 'D', and 10% of its load is distributed to fasteners 'C' and 'E'. The load redistribution for the purlin failure are assumed similar to the fasteners failure.

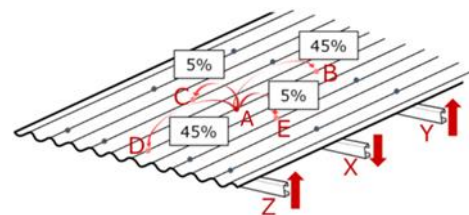


Figure 6. Load sharing percentages (a) Cladding pulling over fixing

The fastener 'A' failure effect is also transferred to the purlins 'Z' and 'Y', increasing the wind load effects on them while decreasing the wind load effect of purlin 'X', as shown in Figure 6. In this model, all the fasteners attached to a purlin section are assumed to be failed when that purlin section is failed.

### Results and Discussion

Vulnerability curves for the industrial buildings in cyclone regions are presented in Figure 7 for a wind direction of  $90^0$ . All the fasteners in the roof are assumed to be without cyclone washers. To investigate the effect of having cyclone washers fitted to the roof, analysis was done for the industrial building fitted with cyclone washers in the roof and these vulnerability curves are plotted in the same figure (Figure 7). A roof sheet is assumed to be failed when 20% of its fasteners have failed. Note that the vulnerability curves plotted in Figure 7 show the averages of percentage roof damage and are based on 10,000 Monte-Carlo simulations.

The results show that vulnerability of an industrial building increases due to a dominant opening. A dominant opening can be created mainly by failure of closed roller doors (Henderson and Ginger, 2008). According to Figure 7, in the building with no

dominant openings the roof damage starts at a wind speed of 80 m/s. A dominant opening reduces the roof damage threshold wind speed to 62 m/s (i.e. dropped by 22%). The main cause for this is the increase in internal pressure of the building in the latter case, thereby increasing the wind load. According to Figure 4, the internal pressure coefficients in an undamaged building are changed from 0 to +0.7 for the building without and with dominant opening respectively.

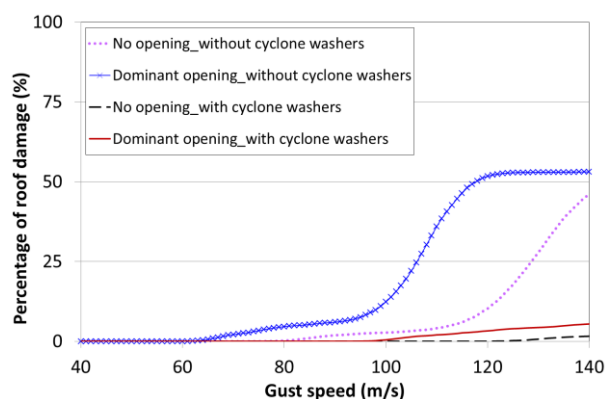


Figure 7. Vulnerability curves for the industrial building

For the industrial building with dominant opening, a low increase in roof damage is observed as the wind speed increases from 62 m/s to 95 m/s. This low accumulation of damage is mainly due to the internal pressure reducing from +0.7 to -0.2 (Figure 4) as a result of roof sheeting failure. Reduction in the internal pressure reduces the rate of wind load increase despite an increasing wind speed. Roof damage percentage is almost constant around 52% beyond a wind speed of 120 m/s with dominant opening (Figure 7). According to Figure 3,  $C_{pe}$  varies between -0.14 and -1.97 and around 50% of the roof area is below  $C_{pe}$  of -0.4. The  $C_{pe}$  of the rest of the area changes from -0.4 to -1.97. The reason for the roof damage to remain almost constant from 120 m/s is the increase in the wind load until the wind load reaches a higher value to fail the remaining fasteners with a  $C_{pe}$  of less than -0.4. Similar reasoning can explain the lower increment in the roof damage from the wind speed  $80\text{ms}^{-1}$  to  $115\text{ms}^{-1}$  in Figure 7 for the industrial building without a dominant opening.

Comparing the vulnerability curves of the industrial building fitted with and without cyclone washers in the roof show that the wind damage is much lower even in higher wind speeds with cyclone washers, irrespective of a dominant opening in the building (i.e. 2% and 5% of roof damage at the wind speed of 140 m/s for the building fitted with cyclone washers with a dominant opening and without a dominant opening, respectively). This shows the importance of having cyclone washers in an industrial building against extreme wind events. The reason for less increase in wind damage of the building fitted with cyclone washers is internal pressure reduction as a result of roof sheeting failure as explained above. When comparing the effect of having a dominant opening in the industrial building fitted with cyclone washers in the roof, Figure 7 shows that the roof damage vulnerability is higher for the building with a dominant opening. Similar results were obtained for the building without cyclone washers as explained above.

## Conclusions

A wind vulnerability model is being developed to predict the probability and extent of damage to metal-clad industrial buildings due to extreme wind loading. The model considered the spatial probabilistic characteristics of wind load and component strength, and load sharing of failed components for the roof envelope. Features such as load sharing and internal pressure

variation are included in this vulnerability model. Vulnerability curves are developed for the representative industrial building (i.e. hot rolled structural steel, metal-clad, gable-end, industrial shed) in cyclonic regions of Australia which is designed to current Australian building standards. Preliminary results were obtained for one wind direction ( $90^\circ$ ). Results show that the importance of using cyclone washers to reduce the vulnerability of industrial buildings due to extreme wind events. It was also found that large internal pressures caused by a dominant opening result in a higher wind vulnerability.

## References

- AS/NZS 1170.2 (2011) Structural design actions – Part 2: Wind actions, Standards Australia, Sydney
- AS4055 (2012) Wind loads for housing, Standards Australia, Sydney
- AS/NZS 4600 (1996) Cold-formed Steel Structures, Standard Australia, Homebush, Australia
- Clarke M J, Hancock G J (1999) Limit states purlin design to AS/NZS 4600:1996. Mechanics of Structures and Materials, Bradford, Bridge and Foster (eds), Balkema, Rotterdam, The Netherlands, 415–422
- Henderson D J (2010) Response of pierced fixed metal roof cladding to fluctuating wind loads, PhD thesis, James Cook University, Australia
- Henderson D, Ginger J (2005) Vulnerability of JCU Group 4 House to cyclonic wind loading, CTS Report TS614 for Geoscience Australia
- Henderson D, Ginger J (2007) Vulnerability model of an Australian high-set house subjected to cyclonic loading. Wind and Structures, 10(3): 269–285
- Henderson D, Ginger J (2008) Role of building codes and construction standards in windstorm disaster mitigation The Australian Journal of Emergency Management, 23(2): 40-46
- Holmes J D (1985) Wind loads and limit states design. Civil Engineering Transactions, Institute of Engineers Australia, 21-26
- Holmes J D (2007) Wind Loading of Structures, Spon Press, London, UK
- Leitch C J, Ginger J D, Henderson D J (2006) Survey of metal-clad, low-rise, low-pitch sheds in cyclonic regions, 12th Australasian Wind Engineering Workshop, Queenstown, NZ
- Pham L (1985) Load combinations and probabilistic load models for limit state codes, Civil Engineering Transactions, Institution of Engineers Australia, CE27, 62-67
- Pham C H, Hancock G J (2009) Direct Strength Design of Cold-Formed Purlins, Journal of Structural Engineering, ASCE, 135(3): 229-238
- Pham L, Holmes J D, Leicester R H (1983), Safety indices for wind loading in Australia, Journal of Wind Engineering & Industrial Aerodynamics, 14, 3-14
- Stewart M G (2014) Risk and economic viability of housing climate adaptation strategies for wind hazards in southeast Australia, Mitigation and Adaptation Strategies for Global Change (in press).
- Stewart M G, Wang X, Willgoose G R (2014), Direct and Indirect Cost and Benefit Assessment of Climate Adaptation Strategies for Housing for Extreme Wind Events in Queensland, Natural Hazards Review 15(4): 04014008(12)